Fuel 397 (2025) 135473

Contents lists available at ScienceDirect

Fuel

journal homepage: www.elsevier.com/locate/fuel

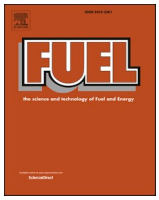

Full Length Article

A novel method for identifying oil content and moveable thresholds in heterogeneous shales

Huiyi Xiao [a,b], Tao Hu [a,b,*], Xiongqi Pang [a,b,*], Chenxi Ding [b], Yunlong Xu [c], Sijia Zhang [a,b], Yao Hu [a,b], Caijun Li [a,b], Tianwu Xu [c], Dingye Zheng [d], Shu Jiang [e], Maowen Li [d]

[a] State Key Laboratory of Petroleum Resources and Engineering, China University of Petroleum (Beijing), Beijing 102249, China
[b] College of Geosciences, China University of Petroleum (Beijing), Beijing 102249, China
[c] Exploration and Development Research Institute, Zhongyuan Oilfield Company, SINOPEC, Puyang 457001, China
[d] Exploration and Development Research Institute, SINOPEC, Beijing 100083, China
[e] Key Laboratory of Tectonics and Petroleum Resources, China University of Geosciences, Ministry of Education, Wuhan 434100, China

ARTICLE INFO

Keywords:
Shale oil content
Heterogeneous shale
Oil moveable threshold
Oil rich threshold
Grading evaluation

ABSTRACT

The exploitation of shale oil is one of the most crucial strategies for alleviating energy shortages, and identifying high-quality oil content sweet spots is a top priority. The common oil content evaluation models typically apply a relatively fixed oil rich threshold and an oil moveable threshold as constraints. However, the high degree of heterogeneity of terrestrial shales means that the accuracy and practicality still require improvement. Here the ΔQ value was introduced to distinguish whether the shale is receiving or expelled hydrocarbon, and validated the comparison using geologic and geochemical data from these two types of shale. Based on the realization that hydrocarbon-accepting shales have high oil content and mobility, first-level and second-level oil quality thresholds are divided and identified, which represent the boundaries of oil quality from poor to good. The application of this model was demonstrated using 225 continuously cored shale samples from the Shahejie Formation of the Dongpu Depression in the Bohai Bay Basin. The results showed that three resource quality tiers were defined: high-quality (S1 $\geq$ 3.77 mg/g & OSI $\geq$ 235 mg/g TOC, 12 % of total resources), medium (0.75 mg/g $\leq$ S1 $<$ 3.77 mg/g & 94 mg/g TOC $\leq$ OSI $<$ 235 mg/g TOC, 32.44 % of total resources) and poor (S1 $<$ 0.75 mg/g & OSI $<$ 94 mg/g TOC, 55.56 % of total resources). ΔQ can be used as a constraint to quickly and accurately identify the oil quality threshold for strongly heterogeneous shale, thus avoiding the complex process of analyzing the influencing factors. In addition, this study found that high-quality shale oil is generally found in received hydrocarbon shale, which mainly exhibit laminated-carbonate lithofacies, and a high frequency interlayering or fracture development. In particular, the expelled hydrocarbon shale's hydrocarbon generation potential and expelled hydrocarbon efficiency together determine oil quality. Overall, this study is expected effectively reduce potential shale oil exploration risks.

1. Introduction

Because of the increasing scarcity of conventional oil and gas resources, the dominant role of oil and gas as primary energy sources is largely sustained by the contributions of shale oil and gas reserves [1,2]. Shale oil can be defined as the petroleum resources contained in shale-dominated formations [3–6], the total recoverable resources worldwide are estimated to be approximately 251.2 billion tons [7]. Although shale oil is very widely distributed and has significant total resources, its actual production capacity is highly variable. Therefore, identifying high-quality oil content sweet spots is a top priority [4,8–14]. Specifically, China's current shale oil occurs mainly in terrestrial basins, where strong heterogeneity of shale leads to greater variability in oil content quality [4,15–19].

Shale oil content quality includes oil content and oil movability, both of which are indispensable for a viable unconventional petroleum system [19–28]. The oil content of shale oil is frequently determined using rock pyrolysis, and the organic matter is heated at different rates and the

Abbreviations: TOC, Total organic carbon; OSI, Oil Saturation Index.

* Corresponding authors.
E-mail addresses: thu@cup.edu.cn (T. Hu), pangxq@cup.edu.cn (X. Pang).

https://doi.org/10.1016/j.fuel.2025.135473
Received 12 December 2024; Received in revised form 23 March 2025; Accepted 21 April 2025
Available online 25 April 2025

amounts of evolved hydrocarbons are measured [15]. The oil content is determined using the S1 (hydrocarbons already generated in shale), TOC (Total Organic Carbon), while the OSI (Oil Saturation Index: S1/TOC, Jarvie, 2012) is used extensively to characterize movability [11,15]. However, there are two issues with this approach [27,29–31]: (1) Using only S1 and TOC as single-element constraints makes it challenging to accurately determine oil content and movability. For example, low TOC represents low hydrocarbon potential, but may contain a large amount of movable oil due to migration, while high TOC may have low oil content due to hydrocarbon expulsion. Even with the same S1 value in different shales, the movable fraction can vary significantly due to differences in mineral composition and pore structure. (2) Although OSI can indicate movability, it has been demonstrated that the S1 and TOC of terrestrial shales are extremely heterogeneous. As a result of this heterogeneity, the movable capacity of shale oil in different regions can be highly variable, particularly under conditions of low TOC and low S1, where significant uncertainty exists. In highly heterogeneous shales the pore structure, hydrocarbon generation parent material, mineral composition, and thickness of sources and reservoirs can significantly affect hydrocarbon movability, and as a result it is currently impossible to correlate the fixed OSI values to real and moveable threshold of shale oil in different areas.

To address the problem of shale heterogeneity, Lu et al. proposed the use of S1 versus TOC plots to evaluate shale oil in a grading manner, including enriched resources, less efficient resources, and inefficient resources. After that, Li et al. and Hu et al. introduced the OSI index in the plots to characterize the movability of shale oil [27,29]. However, the OSI of 100 mg/g TOC that has been proposed for marine shale oil (primarily in tight reservoirs) was commonly used as the oil moveable threshold [11]. The oil rich threshold was often determined based on empirical S1 values or envelope of a series of S1 values. The above method ignores the potential hydrocarbon generation capacity in shale, as well as there is a large uncertainty in the oil movable threshold versus the rich threshold. Previous studies have explored oil moveable thresholds for shales of different maturities, including the use of the hydrocarbon expulsion trends to determine the oil moveable threshold [30], and oil movable threshold grading based on multistep pyrolysis [31]. However, shale oil is distributed within a narrow window of oil generation and there is little variation in maturity in an individual interval at the time of exploration. The identification of oil moveable threshold is based on the understanding that the source rock only undergoes hydrocarbon generation and expulsion processes.

At the same time, scholars have found that oil in heterogeneous shales undergoes frequent micromigration, and hydrocarbons generated in organic-rich shales migrate between lamina and interlayer under the effect of hydrocarbon pressurization and capillary force difference [21,32–39], and shale oil migrates vertically across layers through high-angle fractures [38]. The micromigration of hydrocarbons implies that shale has the property of receiving hydrocarbons as well as expelling hydrocarbons, and the micromigration reflects the combined results of shale oil generation, expelled, and enriched under the control of source-reservoir combination [19]. In general, received hydrocarbon shale have higher oil content due to better reservoir properties [22], and expelled hydrocarbon shale have better mobility due to more light components as a result of migration fractionation effects [20,40–42]. In summary, a more accurate method is needed for the identification of shale oil content quality thresholds, but the use of too many parameters should be avoided.

Dongpu Depression has experienced long-term oil and gas exploration, and the underlying geology is relatively clear. Meanwhile, the shale here shows a thin interlayer overlapping distribution, which provides a good case for us to study the micromigration of shale oil. It first evaluates the micromigration of hydrocarbons through the shale obtained from closely spaced continuous sampling [19], and then determines the oil moveable threshold and oil rich threshold based on the results of hydrocarbon migration under actual geological conditions. At the same time, geological and geochemical analysis methods were applied to verify its accuracy, and discussed its mechanism from the perspectives of hydrocarbon generation, reservoirs, and their combination relationships. This represents the first attempt to establish a shale oil content quality threshold based on hydrocarbon micromigration results and to propose a new evaluation model for it. The results of this study are significant for shale oil exploration in the Bohai Bay Basin and other lake basins around the world.

2. Materials and methods

The samples used in this study were from the shale oil exploration well W410 in the Dongpu Depression, with a total of 225 shale samples taken continuously at intervals of 0.3 m. The target layer is the third member of the Shahejie Formation. Pyrolysis and TOC data were used to analyze the “source” properties of the shale and to establish evaluation models. Rock-eval pyrolysis analyses were performed according to National Standard of China (GB/T 18602-2012) [43]. Samples crushed to $\leq$0.15 mm were analyzed using an OGE-II pyrolyzer. Generated hydrocarbons (S1, mg HC/g rock) were quantified at 300 ℃, followed by programmed pyrolysis (300–650 ℃) to determine potential hydrocarbons (S2, mg HC/g rock) and Tmax (peak hydrocarbon yield temperature). Multistep and freeze–thaw pyrolysis conform to the same standards as conventional pyrolysis but differ in experimental procedure. Fresh rock samples were cryopreserved at −60 ℃ for freeze–thaw pyrolysis, using Cryomill cryogenic grinder and HAWK pyrolyzer to maintain liquid nitrogen temperature (−196 ℃) during crushing. Multistep pyrolysis involved: (1) $S_{1\text{-}1}$ (free hydrocarbons) quantified at 200 ℃; (2) $S_{1\text{-}2}$ (medium-heavy free hydrocarbons) determined via 200–350 ℃ heating; (3) $S_{2\text{-}1}$ (adsorbed hydrocarbons) analyzed at 350-450℃; (4) $S_{2\text{-}2}$ (potential hydrocarbons) measured via 450-600℃ pyrolysis [44]. TOC analyses were performed according to National Standard of China (GB/T 19145-2003) [45]. Samples (~1g) were weighed, ground to <0.2 mm, treated with 1:7 HCl:H_2O to remove inorganic carbon, and analyzed using an LECO CS-744 analyzer.

Core observations, scanning electron microscopy, and mineral composition analysis were used to characterize the “reservoir” properties of the shale. During the sampling process, the shale’s structure and lithology were recorded. Combined with the analysis of the mineral composition of typical samples, lithofacies can be classified on the basis of mineral composition as well as structure. Mineral composition data were obtained based on whole-rock mineral X-ray diffraction (XRD) experiments, which complied with the oil and gas industry standard of China (SY/T 5163-2018) [46]. Samples were oil-washed, crushed to <40 μm, analyzed via Ultima-IV X-ray diffractometer (20 mA, 40 kV, curved graphite monochromator), and XRD spectra used to identify/quantify minerals. Subsequently, a scanning electron microscope (JSM-5500LV) was used to observe the pores and fractures of the shale samples in compliance with the relevant the oil and gas industry standard of China (SY/T5162-2014) [47]. The Rock Casting Image Analyzer (CIAS-2007) is used to observe the pores and fractures of sandstone and other samples in compliance with China’s petroleum industry standards (SY/T6103-2004) [48].

Finally, the nature of the extracts from typical samples was characterized by stable carbon isotopes and gas chromatography of saturated hydrocarbons. Stable carbon isotope analysis involves decomposition, combustion and oxidation of the extracted material, and the purified CO_2 is collected in a sample tube and analyzed for stable carbon isotope composition on an isotope mass spectrometer (DELTAV ADV) (National Standard of China: GB/T18340.2-2010) [49]. The process of saturated hydrocarbons analysis mainly involves chromatographic separation of the saturated hydrocarbon fractions of the extracts in a gas chromatograph (Agilent 6890N), detection of the successive fractions by a hydrogen flame ionization detector, and calculation of the relative percent content (National Standard of China: GB/T18340.5-2010) [50].

The workflow for identifying oil content quality thresholds and

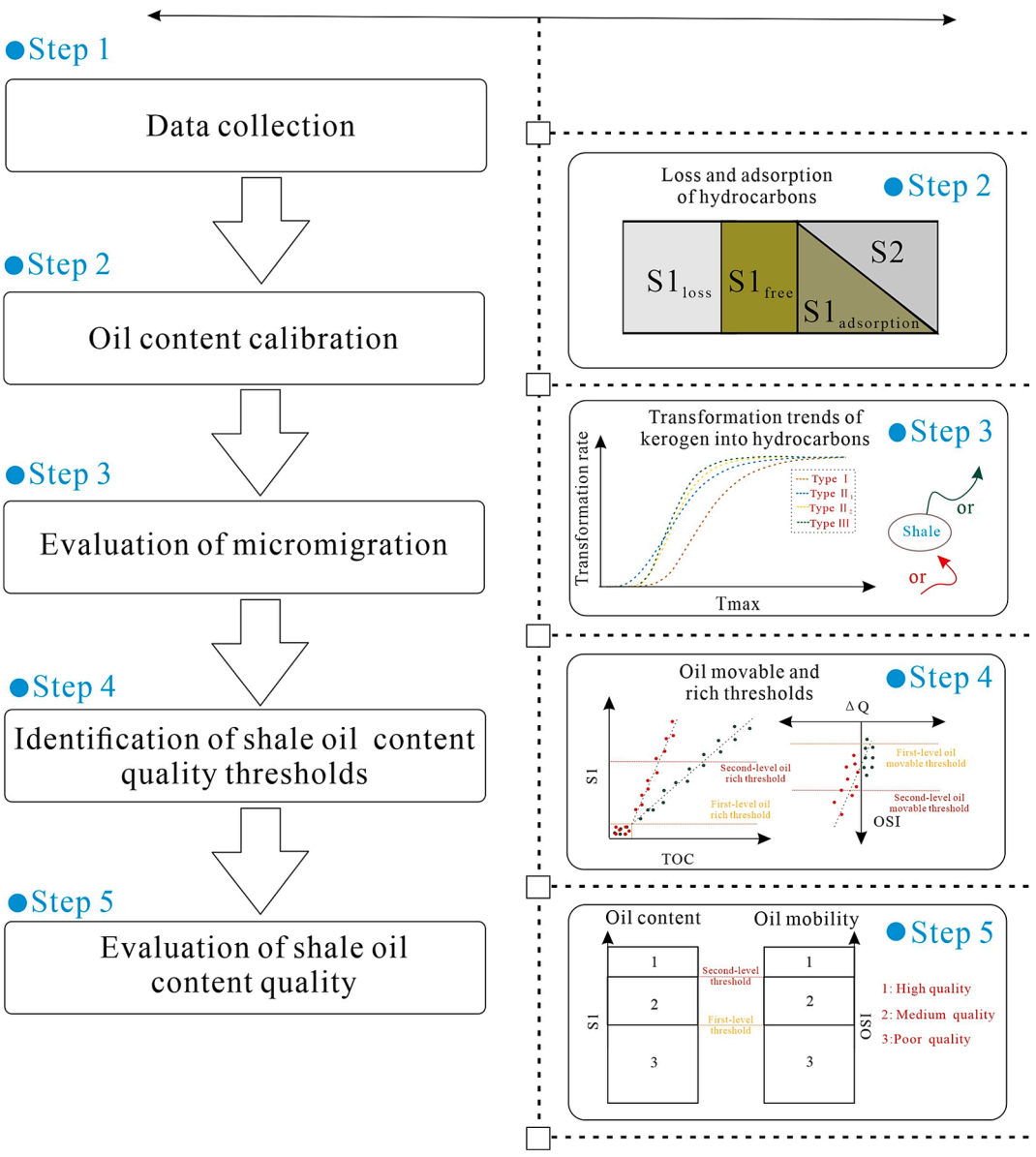

Fig. 1. Workflow for identifying oil content quality thresholds and grading evaluation of shale oil.

grading evaluation of shale oil comprises five primary steps: (1) data collection, (2) oil content calibration, (3) evaluation of micromigration, (4) identification of shale oil quality thresholds, and (5) shale oil quality evaluation (Fig. 1).

First, after obtaining sufficient shale geochemical data, the oil content needs to be calibrated. The loss of volatile hydrocarbons is an unavoidable phenomenon during sample preservation and pyrolysis experiments. Therefore, the data obtained from current analyses may not reflect the true content [11,19]. The actual S1 content of shale in the subsurface ($S1_0$) should include the measured S1 content, light hydrocarbon lost before pyrolysis analysis ($S1_l$), and heavy adsorbed hydrocarbon detected as S2. In this study, S1 from freeze–thaw pyrolysis is considered to be without light hydrocarbon losses, and $S_{2\text{-}1}$ in the multistep pyrolysis is considered to be adsorbed hydrocarbon. A simple calibration model for light and adsorbed hydrocarbons was developed based on multistep and freeze–thaw pyrolysis analyses (Appendix A).

Second, evaluation of micromigration to distinguish whether the shale is expelled hydrocarbon or received hydrocarbon. The hydrocarbon expulsion potential method proposed by Hu et al. [19] was used for quantitative evaluation of hydrocarbon migration. The main principle of this method is to recover the trend in hydrocarbon expulsion and original generation potential of shale through hydrocarbon generation kinetics driven by a large amount of pyrolysis data; Subsequently, the parameter ΔQ is defined as the difference between the original hydrocarbon potential and the present-day hydrocarbon potential. A ΔQ greater than 0 means that hydrocarbons were expelled, while a ΔQ less than 0 means that hydrocarbons have migrated into the rocks ('received hydrocarbons') (Appendix B).

Third, identification of shale oil content quality thresholds, and first-level and second-level oil quality thresholds are divided and identified, which represent the boundaries of oil quality from poor to good. With increasing TOC, the S1 usually exhibits three separate sets of characteristics [15]. Low TOC shales are generally low in hydrocarbon generation, and when S1 content is also low it indicates generally low storage capacity. In addition, shales exhibit good "reservoirs" when they receive large amounts of external hydrocarbons, in both sandstones or carbonates. The second type is a medium TOC shale, and since adsorbed oil is mainly stored in the organic matter network [9,51,52], shales expelling hydrocarbons usually have self-generated amounts of hydrocarbons that have have satisfied their own adsorption capacity and so

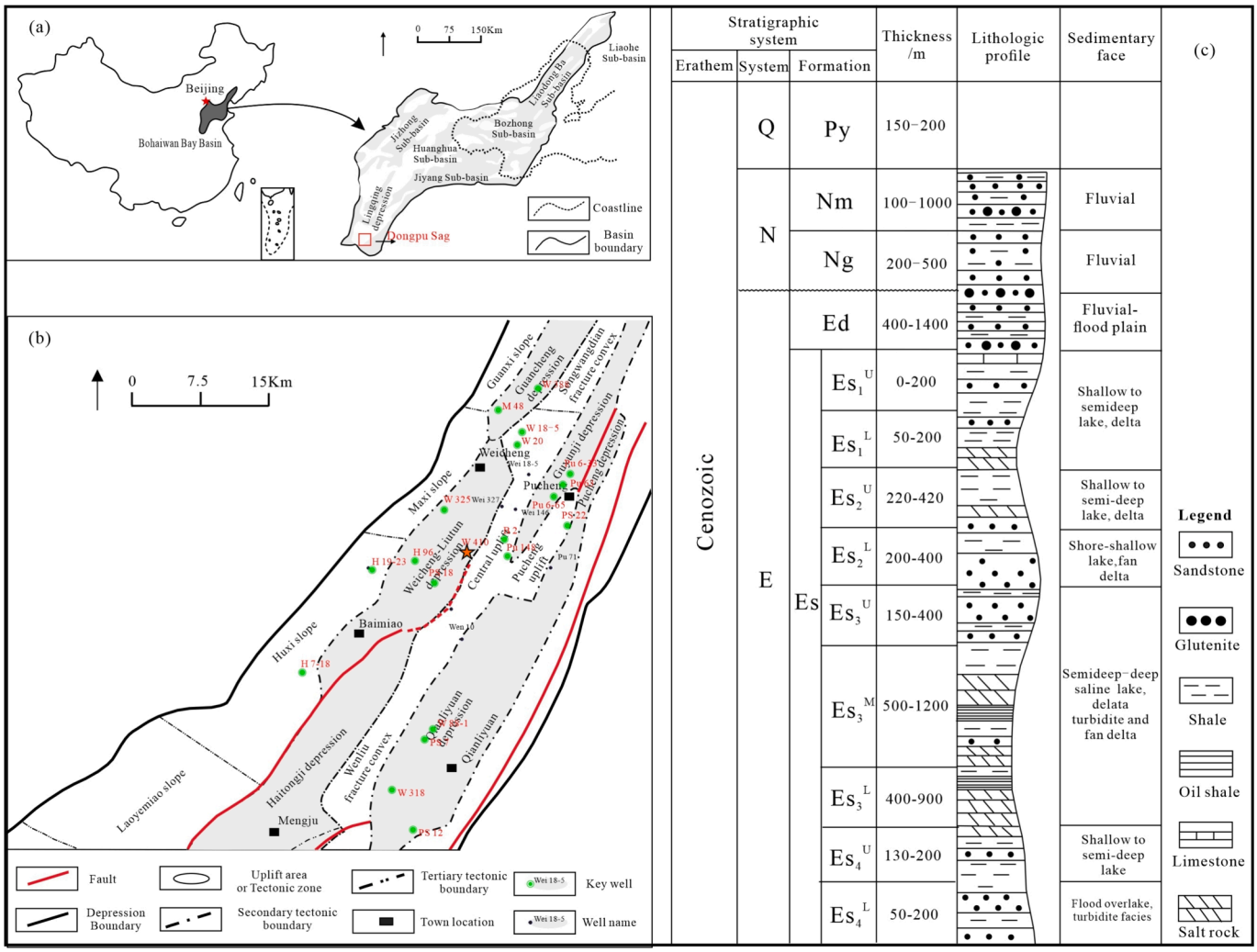

Fig. 2. Geologic map of the Dongpu depression (modified from [53]). (a) Location map. (b) Structural elements. (c) Cenozoic stratigraphic column.

evolve free (i.e., mobile) hydrocarbons (S1). In contrast, shales that have received hydrocarbons usually exhibit higher S1 due to external input of free hydrocarbons. The third type is the shale with high TOC, the hydrocarbon are expelled represents the hydrocarbons in its own reservoir reach the threshold, S1 is not increasing with the hydrocarbon expelled to the outside; and receiving hydrocarbon shale due to the relatively excellent reservoir performance, the increase self-generated free hydrocarbons may result in the continuous increase of S1. The S1 value was used as a measure of oil content, using the S1 of the mixed distribution of expelled and received hydrocarbon samples as first-level oil rich threshold. At the same time, the TOC value at this point represents the potential hydrocarbon generation organic matter abundance (High TOC means there is some potential to generate hydrocarbons in the future). The S1 average of the receiving hydrocarbon samples that enter first-level oil rich threshold were used as second-level oil rich threshold because it represents how much oil is in the shale of good storage quality. Furthermore, the minimum OSI was used for shales that have effectively stored hydrocarbons (greater than first-level oil rich threshold) as the first-level oil moveable threshold and the average of migrated hydrocarbons (ΔQ less than 0) as the second-level oil moveable threshold because they represent the ability of the hydrocarbons to undergo migration under actual geologic conditions.

Fourth, the content quality of shale oil was evaluated by considering two main attributes: oil content and oil movability. Two parameters above the second-level threshold can be categorized as high-quality resource. Two parameters above the first-level threshold are categorized as medium resource, which includes the subcategories of medium-enriched and movable resource, enriched and medium movable resource, and medium-enriched and medium-movable resource. For shale oil that has not reached both first-level thresholds, they were categorized as a poor resource, where those with moderate oil volumes but poor movability are categorized as less efficient resource, which are unlikely to be exploited under current conditions. Considering that part of the shale may have large hydrocarbon generation and expulsion potential, and has the potential to be heated in-situ to form shale oil, the part with poor oil content and movability, but with large TOC content, were categorized as a potential resource. Otherwise, shales with both below the first-level threshold are categorized as ineffective resources.

3. Geological setting

The Dongpu Depression is located in the southwestern margin of the Bohai Bay Basin in China, covering an area of about 5300 km^2 (Fig. 2a, b). It is a Cenozoic faulted lake basin with multiple depositional cycles [8,53,54], with a shallow western slope and a steep eastern slope. Over the past few years, several wells have been drilled in the Zhongyuan Field and have obtained significant shale oil flows. In this study, samples of the Shahejie Formation from the W410 well are used as an application example to demonstrate the workflow and results of the new model.

The Shahejie Formation was deposited in a variety of environments, including deltas and shallow to deep lakes, and overall is dominated by

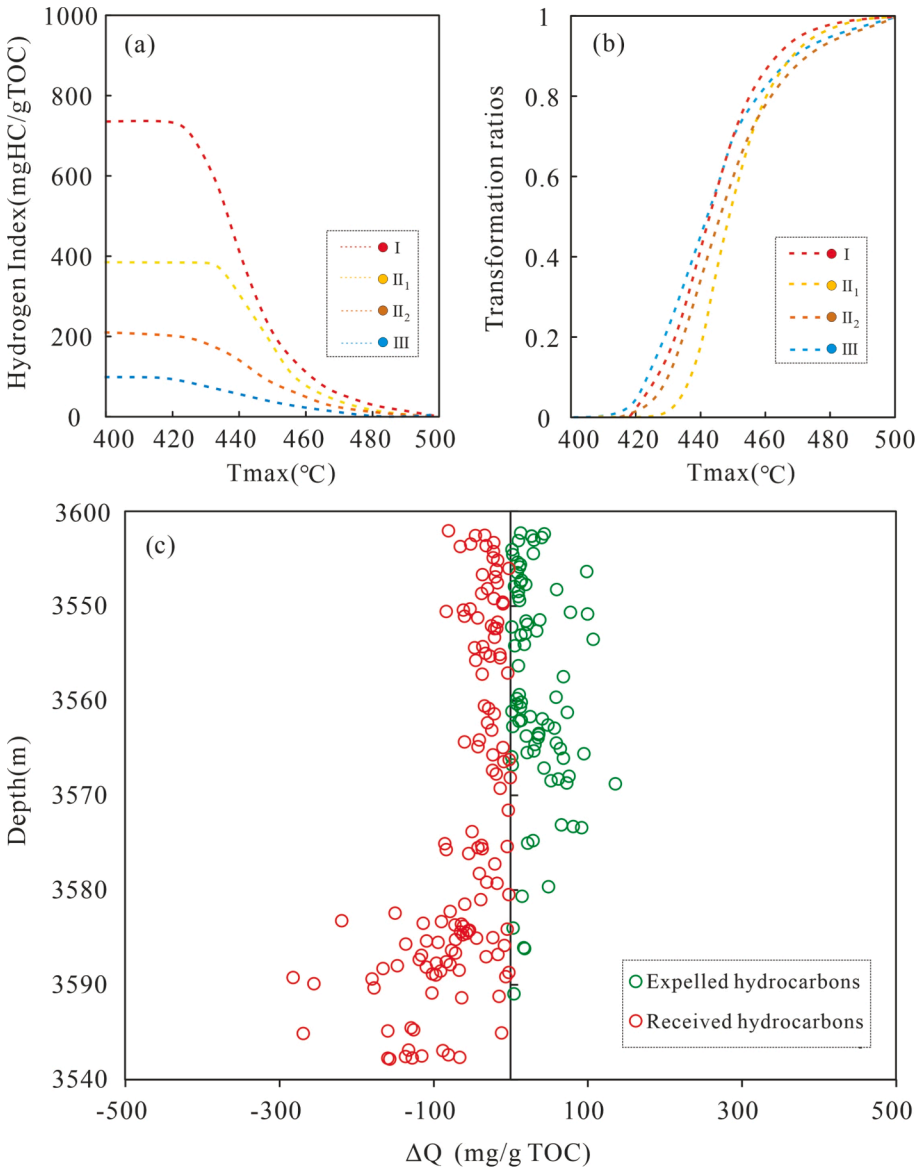

Fig. 3. (a) Evolution of Hydrogen Index and (b) kerogen transformation ratios with increased maturity (modified from [56]). (c) ΔQ of shale at different depths in Well W410.

shales and thin-bedded siltstones formed by changes in high-frequency lake surface [53–55], and is the main hydrocarbon-bearing stratum in the depression (Fig. 2c). Among them, shale is characterized by medium organic matter abundance, Type II kerogen dominance, and medium to high maturity, contributing almost all of the hydrocarbons in the depression, with only a small portion of the natural gas coming from Permian coal-derived source rocks. Therefore, it is the focus of shale oil exploration.

4. Results

Wu et al. [56] developed an evolution model of Hydrogen Index and kerogen transformation ratios with increased maturity applicable to the Dongpu Depression shale based on the method proposed by Hu et al. [19] (Fig. 3a,b). This model was used to calculate ΔQ for the shale in well W410 (Appendix B), and the results showed that 61.5 % of the samples had external hydrocarbon charging, with charging amounts ranging from 0.34 to 282.2 mg/g TOC, with an average of 62.3 mg/g TOC. The remaining 38.5 % of the samples experienced hydrocarbon expulsion, with hydrocarbon expulsion amounts ranging from 1.43 to 135.9 mg/g TOC, with an average of 33.91 mg/g TOC. Overall, the migration of hydrocarbons in the upper half of the sampled interval is frequent but generally weak, while the migration of shale oil in the lower half is mainly dominated by received hydrocarbons, and the intensity can reach more than 100 mg/g TOC (Fig. 3c).

The organic geochemical characteristics of shale are important "source" properties. The analytical results of the sampled of the W410 shale show that (1) the overall shale is of medium–low abundance TOC (Fig. 4a), with TOC contents ranging from 0.15 to 7.67 wt% (average: 0.98 wt%). Both receiving and expelled hydrocarbon samples have a broad TOC distribution, but the overall mass of received hydrocarbons (average: 0.87 wt%) is lower than that of expelled hydrocarbons (average: 1.18 wt%). (2) Organic matter types were mainly distributed between Type II_1 and Type II_2, although a significant concentration of Type III was also observed in this continuous sampling analysis, and was characterized by a significant amount of received hydrocarbons and low abundance TOC (Fig. 4b). (3) Organic matter maturity is mainly distributed in the low maturity stage, and the measured Ro is between 0.7 % and 0.85 %.

The carbonate lithofacies and laminated lithofacies shales of the

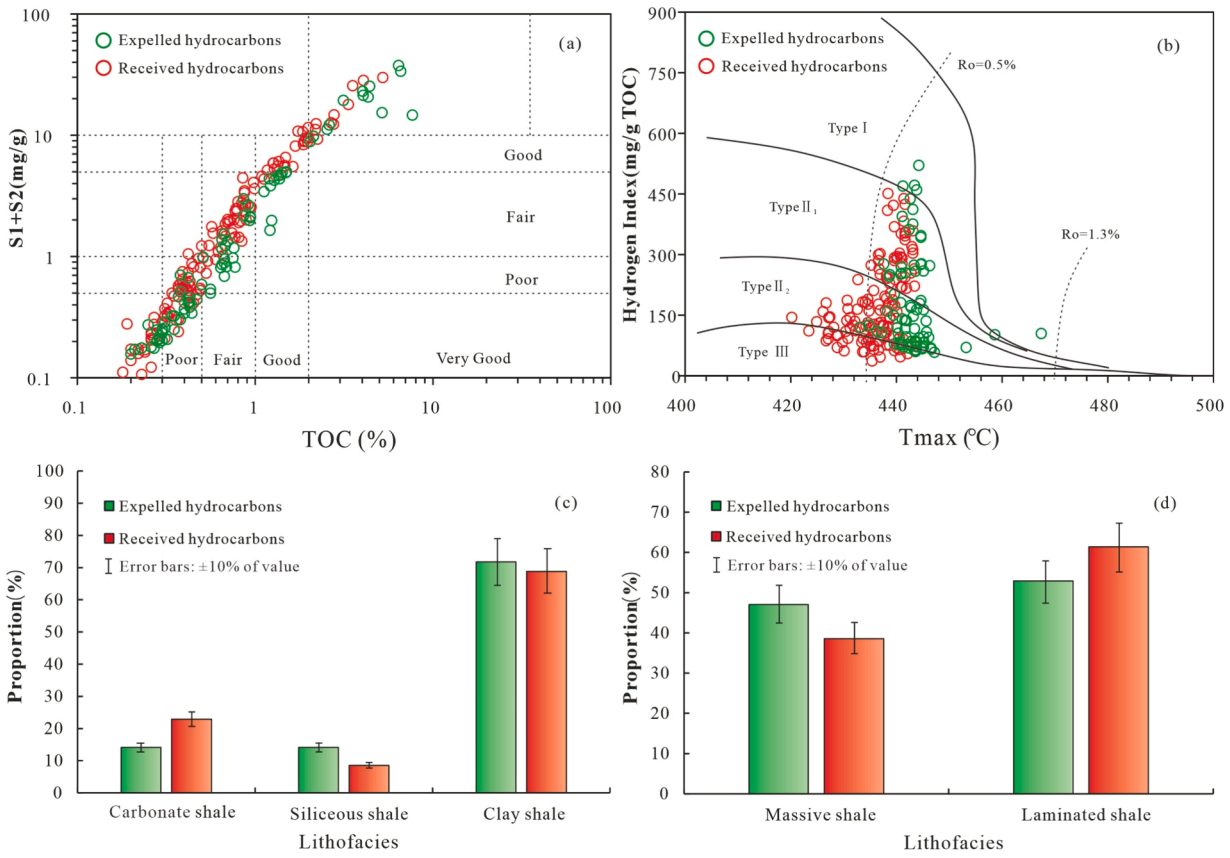

Fig. 4. Source and reservoir properties of shale from well W410. (a) Plot of S1 + S2 contents versus TOC content. (b) Plot of Hydrogen Index versus Tmax. (c) Proportions of carbonate shale, siliceous shale, and clay shale.(d) Proportions of massive shale and laminated shale.

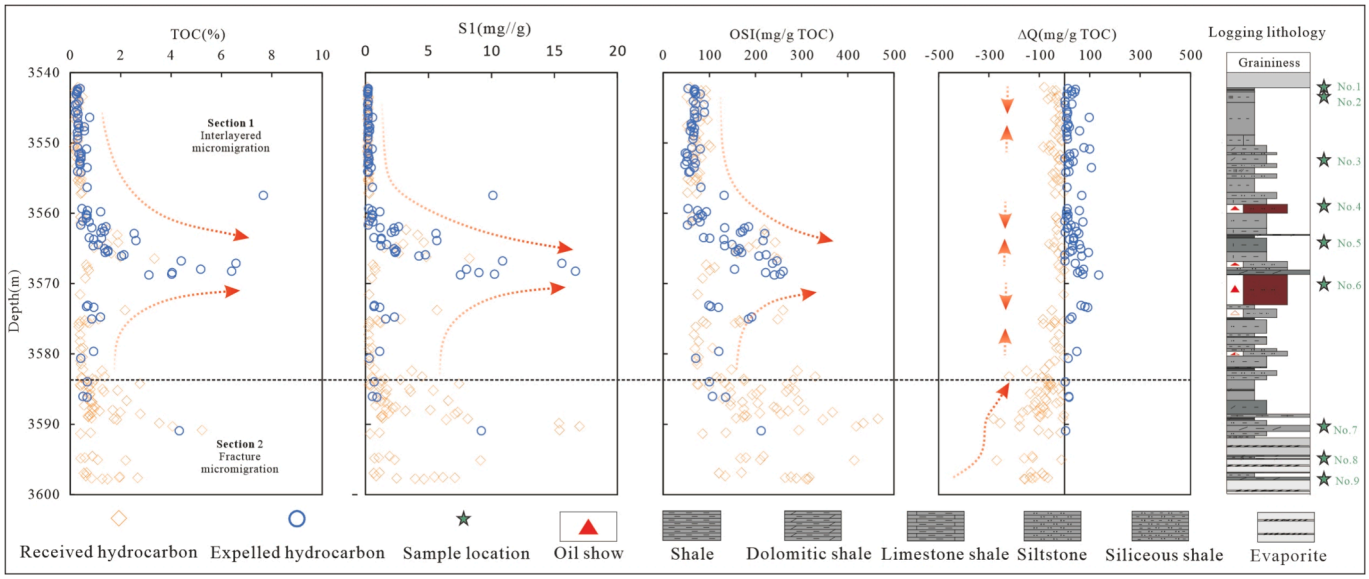

Fig. 5. Vertical profile of TOC, S1, OSI, ΔQ and lithology lithological characteristics in shale from well W410.

Dongpu Depression are favorable types for oil storage, and the pore structures are generally controlled by carbonate minerals and organic matter [53,57,58]. Statistical analysis of the core observations revealed that the proportion of carbonate lithofacies in the receiving and expelling hydrocarbon shale is 23 % and 14 %, respectively, and that the carbonate shale lithofacies in the receiving hydrocarbon shale account for 73 % of the total carbonate shale lithofacies (Fig. 4c). Meanwhile, the proportions of laminated lithofacies in the receiving and expelling shales are 61 % and 53 %, respectively, and the laminated lithofacies in the receiving shale account for 66 % of the total amount of laminated shale lithofacies (Fig. 4d); these results indicate that the storage performance of the receiving shale is relatively good compared with that of the expelling shale.

The vertical distribution of the ΔQ shows that the migration of

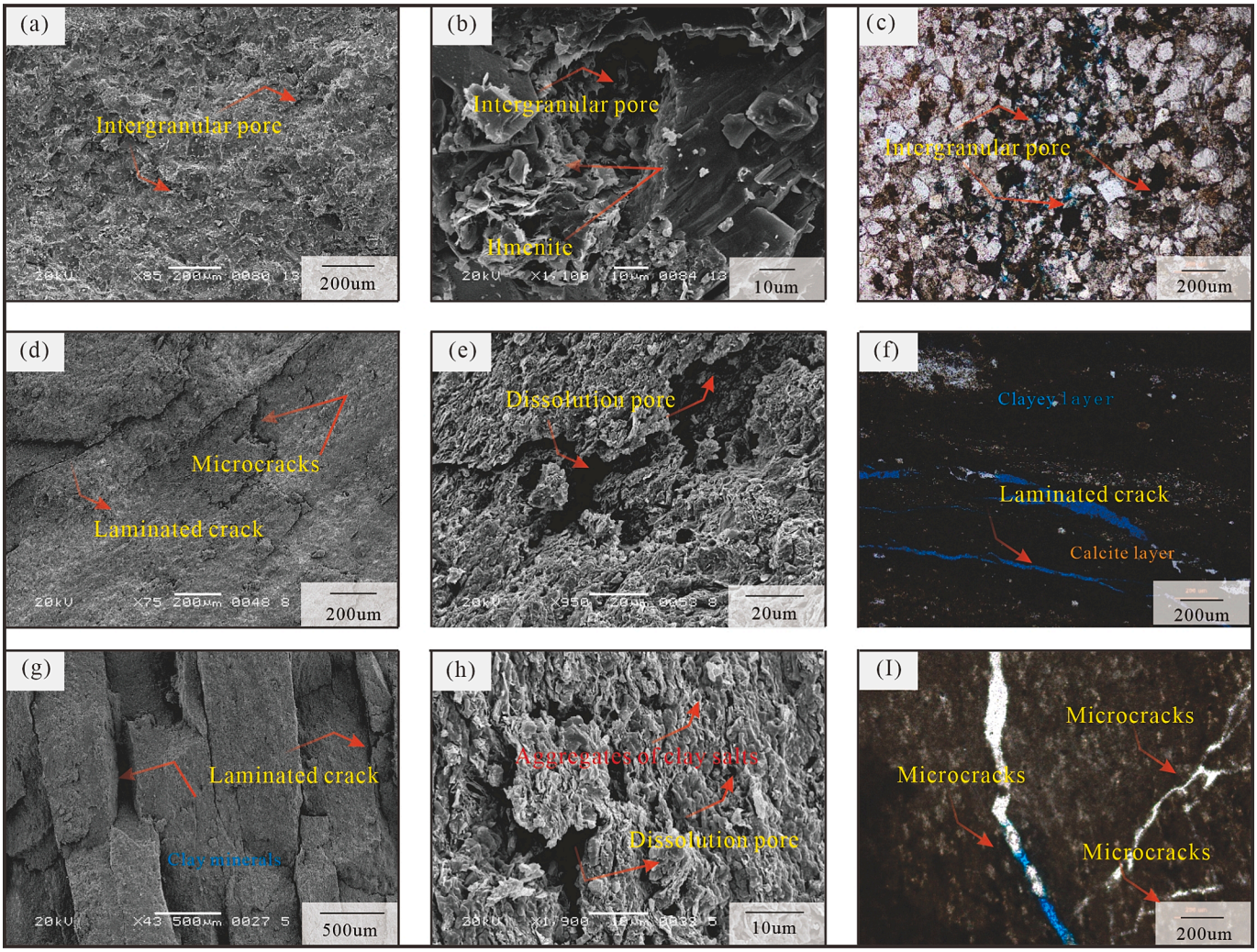

Fig. 6. Microscale pore-fracture microscopic images of different lithology samples from well W410. (a) 3566.62 m, siltstone, intergranular pores. (b) 3566.62 m, siltstone, intergranular dissolution pores. (c) 3558.73 m, siltstone, pores patchy distribution, visible microfractures. (d) 3562.33 m, shale, laminations fractures developed. (e) 3562.33 m, shale, dissolution pores. (f) 3563 m, shale, occasional fine pores, microfractures developed. (g) 3582.43 m, shale, laminated fractures. (h) 3582.43 m, shale, dissolution pores. (i)3589.85, dolomite, tectonic microfractures.

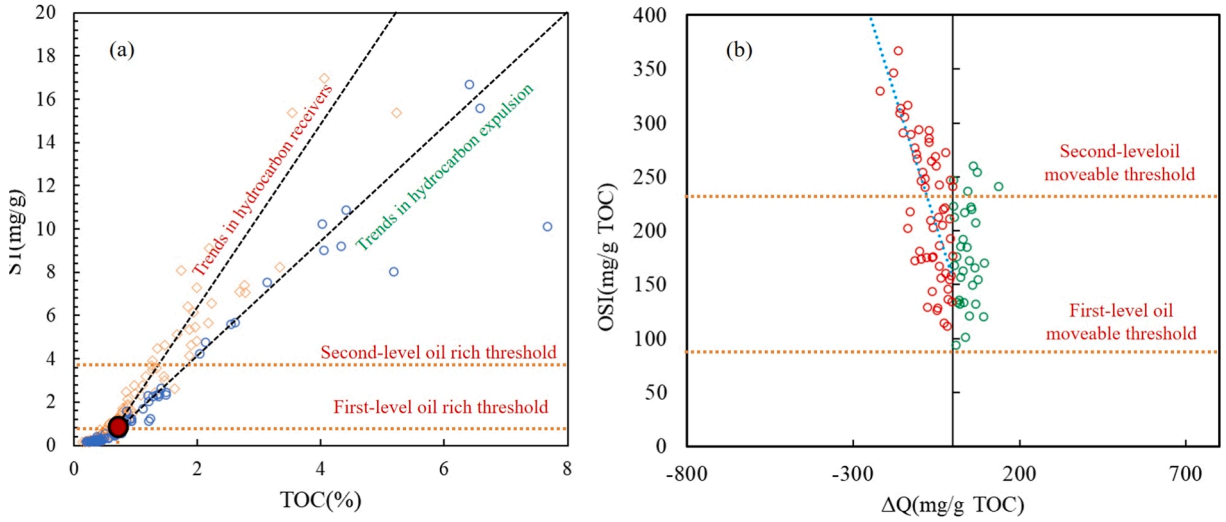

Fig. 7. Oil content quality thresholds for shale of well W410. (a) Determination of oil rich threshold based on S1 versus TOC plot. (b) Determination of oil moveable threshold based on OSI versus ΔQ plot.

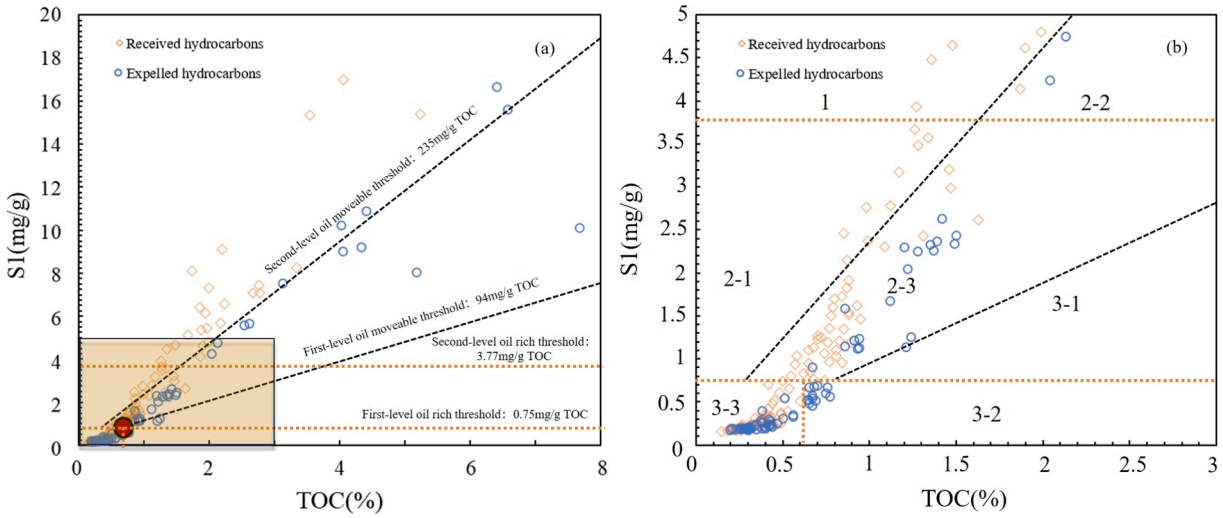

Fig. 8. (a) Relationship between the S1 content and TOC for various types of shale oil and (b) local zoomed-in figure, the specific extent of the color-filled area of (a) (Note: 1-High-quality resource; 2-Medium resource; 3-Poor resources; 2-1-Medium-enriched and movable resource; 2-2-Enriched and medium-movable resource; 2-3-Medium-enriched and medium-movable resource; 3-1-Less efficient resource; 3-2-Potential resource; 3-3-Inefficient resource).

hydrocarbons is highly dependent on the spatial configuration of sources and reservoirs, which is manifested in three characteristics (Fig. 5). First, the short distances over which shale oil is migrated and the interbedding of facies with expelled hydrocarbons with those containing received hydrocarbons. Second, the siltstone with good oil and gas indications is usually adjacent to the occurrence of high-quality shale, as shown in section 1 of Fig. 5, the upper part of the shale is of poor quality, and consequently the siltstone usually has no oil and gas show, while the siltstone at the top and bottom of the high-quality shale has oil and gas show. Third, the continuous hydrocarbon-receiving shale sections with better reservoir properties usually show fracture development, and in section 2 hydrocarbon-receiving shale and fractures are commonly developed.

Observation of microscopic images reveals that both siltstone and shale are generally tight, with it is difficult to migrate fluids into the pores. The pore space of sandstone is relatively developed, with intergranular pores and dissolution pores visible, while the observable pore space of shale is relatively poor, being dominated by microfractures and laminar fractures (Fig. 6). This also explains why shale oil typically has short micromigration distances and better hydrocarbon shows in adjacent siltstones (Fig. 5).

The plot of S1 versus TOC exhibits a bipartite trend (Fig. 7a), and it is

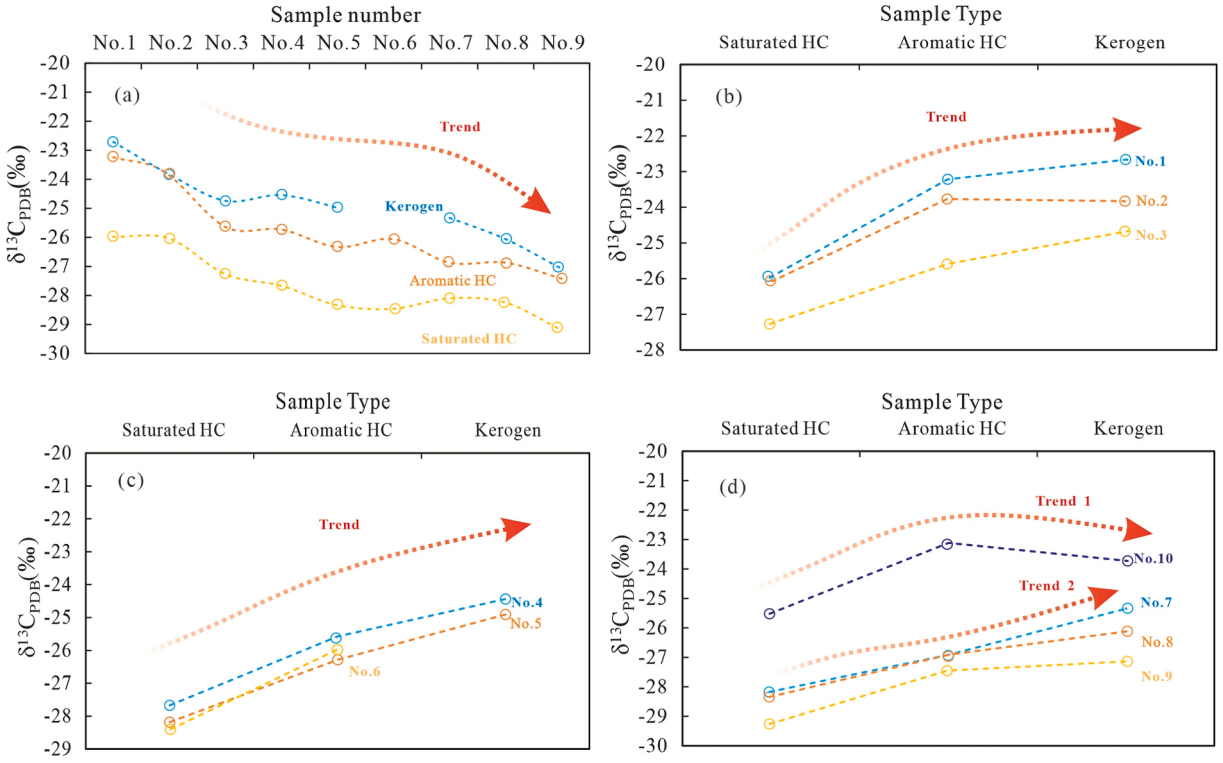

Fig. 9. Carbon isotopic characterization of extracts from typical samples (See Fig. 5 for sample locations,and the depth is increasing from No. 1 to No. 10). (a) Overall characteristics. (b) Samples in the upper half of the interlayer micromigration model. (c) Samples in the lower half of the interlayer micromigration modes. (d) Samples in the fracture micromigration interval.

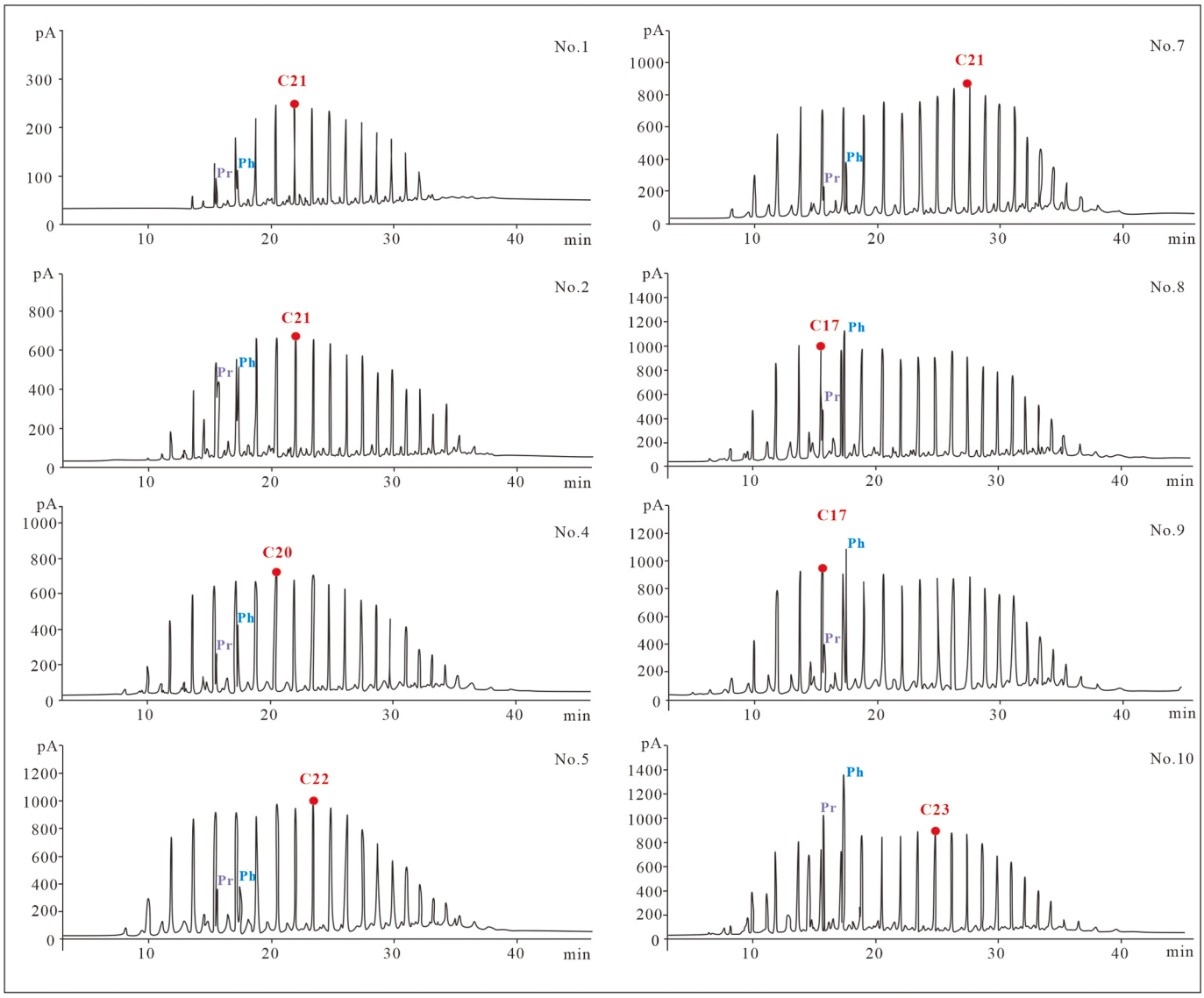

Fig. 10. Saturated hydrocarbon distributions of typical samples (See Fig. 5 for sample locations, and the depth is increasing from No. 1 to No. 10).

difficult to distinguish between hydrocarbon-receiving and hydrocarbon-expelling shales when TOC is less than 0.65 % and S1 is less than 0.75 mg/g, which indicates that the hydrocarbon generation and storage capacities of these shales are generally low. Using this relationship, first-level oil rich threshold was identified with S1 = 0.75 mg/g and TOC = 0.65 wt%. The average oil content of the samples entering first-level oil rich threshold was calculated to be 3.77 mg/g, corresponding to second-level oil rich threshold (Fig. 7a). The minimum OSI of the samples entering first-level oil rich threshold for first-level oil moveable threshold was determined as 94 mg/g TOC via OSI-ΔQ analysis, whereas the mean OSI of hydrocarbon-receiving samples for second-level oil moveable threshold was determined as 235 mg/g TOC (Fig. 7b).

Using oil moveable threshold and oil rich threshold as constraints, out of 225 samples, the percentages of the three different levels of resources, high-quality resources, medium resources, and poor resources, were 12 %, 32.44 %, and 55.56 %, respectively. Ineffective resources (49.33 %) in poor resources and moderately rich and moderately movable resources (24.44 %) in medium resources accounted for the largest share of these resources (Fig. 8a). These results indicate that the shale oil from well W410 is extremely heterogeneous, with very large variations in the quality of the oil content and a large percentage of poor resources. In addition, it was found that almost all of the high-quality resources are received hydrocarbon shale, and 64 % of the medium resources are received hydrocarbon shales (Fig. 8b).

5. Discussion

Evaluation results reveal two distinct migration modes (Fig. 5): interlayer migration (Section 1) and fracture migration (Section 2). The carbon isotopes of saturated hydrocarbons, aromatic hydrocarbons, and kerogen in samples show similar trends with depth (Fig. 9a), which implies that the hydrocarbons have not been migrating over long distances [41]. For samples within the Section 1 interval, which at adjacent depths show a high degree of homogeneity (Fig. 9b, c). However, the fractures may have contributed to some cross-layer migration of shale oil. Samples no. 7–9 have similar isotopic signatures and are distributed in Section 2 interval, but an intersection between 7 and 8 was observed, and they differ from the trend of 9–10, which implies that they may have been formed from a mixed source (Fig. 9d). Samples no. 7–9 are also shown to have lighter isotopic masses from Fig. 9a, which corroborates the more active hydrocarbon migration in these shales [20,42]. Further analysis of the saturated hydrocarbon chromatograms shows that the neighboring samples in the section 1 show similar characteristics

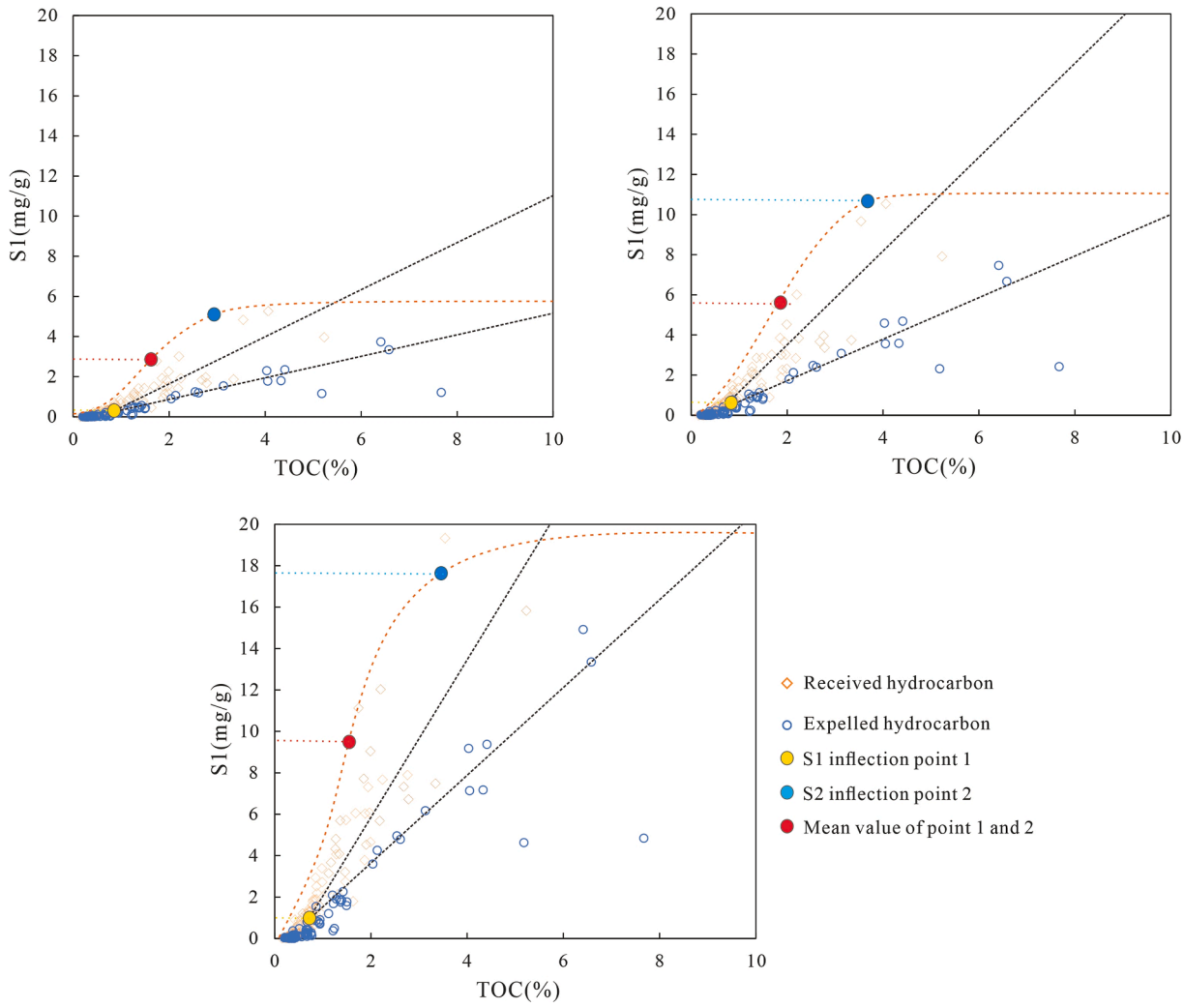

Fig. 11. Plots of oil rich threshold identifications with different calibration coefficients. (a) With a calibration coefficient of 0.5. (b) Without calibration of S1. (c) With a calibration coefficient of 2.

(Fig. 10). On the other hand, the chromatograms of sample in the section 2 all show double-peak characteristics, but No. 7 and No. 10 are dominated by the higher molecular weight peaks, while No. 8 and No. 9 are dominated by the anterior peaks (Fig. 10). The above results indicate that the presence of fractures may have allowed mixing of hydrocarbons from different sources.

Micromigration refers to the migration and re-distribution of hydrocarbons within shale formations, which includes the retention of hydrocarbons from self-generation and external sources. First of all, in the shale that receives hydrocarbons, the "reservoir" is larger than the "source", which means that this shale has more space to store hydrocarbons. However, when the quantity of the received hydrocarbons is larger, it means that this kind of shale oil has more light components, which are a current priority in shale oil exploration [18,19,21,23,24,41]. Hydrocarbon expulsion occurs in shales when the intensity of hydrocarbon generation capacity is greater than the storage capacity. It means that its hydrocarbon supply capacity is higher, and it can be a potential shale oil target layer, because it may still contain a large amount of residual hydrocarbons and organic matter that has not yet been transformed into hydrocarbons [18,21,33,34,59,60]. The results of the shale oil grading evaluation show that 81 % of the high quality shale oil resources are in received hydrocarbon shale. In view of different migration modes, 67 % of the high-quality resources are distributed in the fracture migration interval. This means that ΔQ can be used to reflect the quality of shale oil content when no suitable grading model has been developed. At the same time, these two proportions were 64 % and 51 % for medium resources. Further analysis indicates that 67 % of the medium resources in the interlayer migration interval are expelled hydrocarbon shales, which indicates that the resources in expelled hydrocarbon shale should not be ignored. Statistical analyses based on medium resources indicate that in expelled hydrocarbon shale compared to received hydrocarbon shale generally have higher S1, but relatively lower OSI (Fig. 8). The quality of hydrocarbon-receiving shale oil is controlled by reservoir properties, while the occurrence of sufficient oil content is a key factor. It appears that inorganic minerals are more conducive for inorganic pore formation, and fractures enhance the connectivity of the reservoir space [34,35,38]. The quality of hydrocarbon-expelling shale oil needs to focus on content and movability. The shale's hydrocarbon generation potential and expelled hydrocarbon efficiency together determine oil quality, which is higher when it generates large amounts of hydrocarbons but is retained, so the Type II kerogen may contain more moveable residual hydrocarbons due to the fact that hydrocarbons in this type of shale are generated in sufficient quantities and do not expell in large quantities [27,30,31].

In the application of the model, the accuracy of the oil content seriously affects the grading of the resources. Samples without S1 correction will have significant effects, which will be illustrated using examples with calibration coefficients of 0.5, 1 and 2 (Fig. 11). First, the overall S1 change will result in a difference in the oil rich threshold, with a higher threshold after calibration. Second, since shale samples with

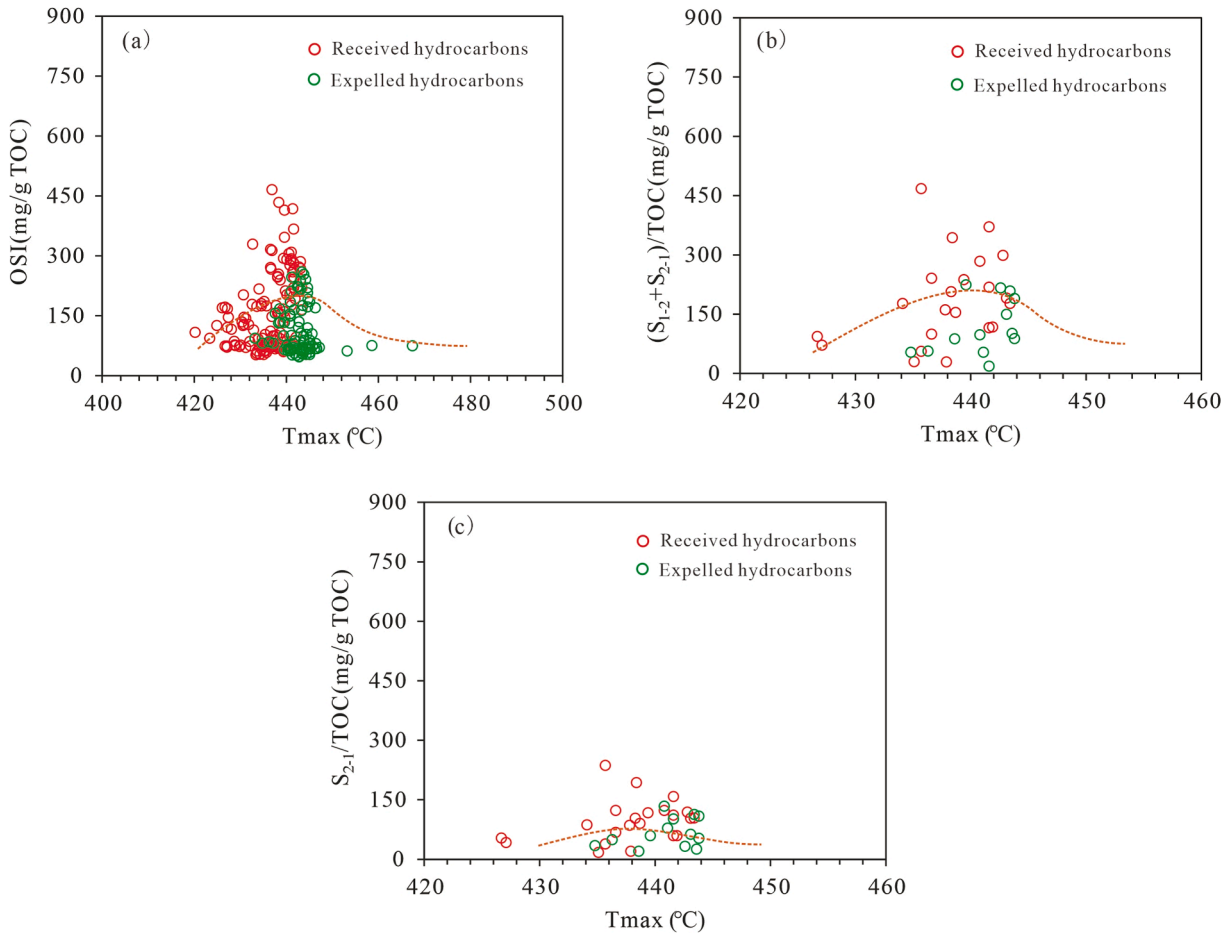

Fig. 12. Oil moveable threshold identification plots derived from (a) OSI versus Tmax [30], (b) (S_{2-1} + S_{1-2})/TOC versus Tmax [31] and (c) S_{2-1}/TOC versus Tmax [31].

high TOC have greater hydrocarbon potential, more hydrocarbons will be dispersed for the same calibration coefficient, which may lead to an inflection point of S1 at high TOC, confusing lost hydrocarbons with expelled hydrocarbons, which will result in a larger error in shale oil resource grade determination. Finally, since light hydrocarbon loss generally does not affect the level of TOC, not calibrating S1 can similarly lead to deviations in oil moveable threshold determination.

Compared with previous models, an assessment of potential resources was included in this mode. In addition, the resource abundance of shales varies widely, making it difficult for traditional classification methods to fully reflect shale oil content quality, and this model provides a method for accurately identifying the oil rich threshold and oil moveable threshold.

The models of Hu et al. [27], Wang et al. [30], and Wang et al. [31] were applied for shale oil quality evaluation, respectively. For the identification results of oil rich threshold, the three previous models used envelopes or empirical values determined subjectively, and the data heterogeneity will result in bias in the oil content level, especially for second-level oil rich threshold (Fig. 8, Fig. 11). For oil moveable threshold, Hu et al. [27] used a fixed OSI value (100 mg/g TOC); however, the calibrated OSI was significantly larger than this threshold. The model of Wang et al. [30] introduced Tmax in order to model variable oil moveable threshold. However, the heterogeneity of the kerogen resulted in a poor correlation between oil moveable threshold and Tmax (Fig. 12a). At the same time, the existence of migration hydrocarbons may lead to particularly large differences in S1 for samples at the same maturity, which further exacerbates the uncertainty in the oil movable threshold. The model of Wang et al. [31] introduced multi-step pyrolysis to characterize the movability. However the higher amount of data (and the subsequent additional cost) limit the applicability to some extent, and again, does not address the effect of hydrocarbon migration on oil moveable threshold (Fig. 12b, Table 1).

The advantages of this model are its simplicity and rapidity. With the rock pyrolysis data, the model is able to grade and evaluate shale oil resources quickly and effectively. This advantage makes it particularly suitable for shale reservoirs that are highly heterogeneous, especially those with rapidly changing oil content quality. Another advantage of the model is that it provides a method to quickly identify the oil quality

Table 1
Comparison of oil moveable and rich threshold under different models for shale oil in well W410.

Threshold	Hu et al.		Wang et al.		Wang et al.		This study	
Oil rich threshold	Name	Value	Name	Value	Name	Value	Name	Value
	S1 (mg/g rock)	0.5–1 4–6	S1 (mg/g rock)	0.5–1 4–6	S1 (mg/g rock)	0.5–1 /	S1 (mg/g rock)	0.75 3.77
Oil moveable threshold	OSI(mg/g TOC)	100 /	OSI(mg/g TOC)	80–175 /	S_{1-2}/TOC (mg/g TOC) (S1-2+S2-1)/TOC (mg/g TOC)	30–100 100–200	OSI (mg/g TOC)	94 235

threshold. In those basins with complex shale structures (sedimentary & tectonic), the oil quality threshold can be identified directly by using the results of the hydrocarbon migration distribution (S1, OSI) in the subsurface, omitting the complexity of source rock, reservoir, and migration conditions. However, in order to make the model as accurate as possible in its application, the creation of the same mode should avoid samples with extreme reservoir or source rock properties, and shale with the same destination layer or with small differences in depth should be selected for evaluation.

6. Conclusions

This study proposes a novel method and model for identifying shale oil moveable threshold and rich threshold, and for grading their quality based on rock pyrolysis parameters. Using continuous cores from the Eocene Shahejie Formation in the Dongpu Depression as a case study, three resource quality tiers were defined: high-quality (S1 $\geq$ 3.77 mg/g & OSI $\geq$ 235 mg/g TOC, 12 % of total resources), medium (0.75 mg/g $\leq$ S1 $<$ 3.77 mg/g & 94 mg/g TOC $\leq$ OSI $<$ 235 mg/g TOC, 32.44 % of total resources) and poor (S1 $<$ 0.75 mg/g & OSI $<$ 94 mg/g TOC, 55.56 % of total resources). Compared to previous rapid identification and evaluation models, ΔQ can be used as a constraint to quickly and accurately identify the oil quality threshold for strongly heterogeneous shale, thus avoiding the complex process of analyzing the influencing factors. In addition, this study found that high-quality shale oil is generally found in received hydrocarbon shale, which mainly exhibit laminated-carbonate lithofacies, and a high frequency interlayering or fracture development. In particular, the expelled hydrocarbon shale's hydrocarbon generation potential and expelled hydrocarbon efficiency together determine oil quality. Overall, this study is expected effectively reduce potential shale oil exploration risks.

CRediT authorship contribution statement

Huiyi Xiao: Writing – review & editing, Writing – original draft, Methodology, Investigation, Data curation. **Tao Hu:** Writing – review & editing, Methodology. **Xiongqi Pang:** Supervision, Methodology, Funding acquisition, Conceptualization. **Chenxi Ding:** Writing – review & editing, Visualization, Software. **Yunlong Xu:** Writing – review & editing, Data curation. **Sijia Zhang:** Software, Methodology. **Yao Hu:** Writing – review & editing, Methodology. **Caijun Li:** Software, Data curation. **Tianwu Xu:** Writing – review & editing, Data curation. **Dingye Zheng:** Writing – review & editing, Methodology. **Shu Jiang:** Investigation, Formal analysis. **Maowen Li:** Writing – review & editing, Conceptualization.

Declaration of competing interest

The authors declare that they have no known competing financial interests or personal relationships that could have appeared to influence the work reported in this paper.

Acknowledgments

This study was financially supported by the National Natural Science Foundation of China, China (U22B6004, 42202133, U24B6002), CNPC Innovation Fund, China (2022DQ02-0106), Key Laboratory of Tectonics and Petroleum Resources of the Ministry of Education, China (TPR-2023-05), National Natural Science Foundation of China, China (41872148, 42072174, 42130803), Strategic Cooperation Technology Projects of the CNPC and CUPB, China (ZLZX2020-01-05), Sinopec Zhongyuan Oilfield and CUPB Cooperation Project, China (31300027-23-ZC0613-0013), AAPG Foundation Grants-in-Aid Program, United States (22272306).

Appendix A

Steps of Oil content calibration

Step 1: Calibration for light hydrocarbon loss. Freeze-thaw pyrolysis is practically free of hydrocarbon losses because the samples are kept at low temperatures during preservation and crushing. The S1 obtained using freeze–thaw pyrolysis can represent the S1c before the loss of light hydrocarbons. For the same sample subjected to both freeze–thaw pyrolysis and conventional pyrolysis at the same time, the relationship equations of conventional pyrolysis S1 and TOC to freeze–thaw pyrolysis S1c can be established:

$$S1c = a1 \times TOC + b1 \times S1 + c1 \quad (1)$$

where, S1c is measured by freeze–thaw pyrolysis and represents the free hydrocarbons before the loss of light hydrocarbons, mg/g. TOC is the total organic carbon (TOC) of the samples, %. S1 is measured by conventional pyrolysis and represents the free hydrocarbons after the loss of light hydrocarbons, mg/g. a1, b1, and c1 are the correlation coefficients and are dimensionless. In this model, a1, b1, and c1 are 0.133, 1.143, and 0.134, respectively.

Step 2: Calibration for adsorbed hydrocarbons. In conventional pyrolysis, there is difficulty in effectively distinguishing between S1 and S2 because some generated heavy adsorbed hydrocarbons (Part of the S1) will be incorporated into the S2. Multistep pyrolysis is an improved method used to determine the free hydrocarbon content ($S_{1\text{-}1}$), pertaining to the light component of free oil present in the connected pores of shale. Further, $S_{1\text{-}2}$ represents the content of medium-heavy components of free oil, $S_{2\text{-}1}$ represents the content of adsorbed hydrocarbons, and $S_{2\text{-}2}$ represents the content of pyrolysis hydrocarbons. Conventional and multistep pyrolysis analyses were performed for the samples and the relationship between S2c ($S_{2\text{-}1}$) and TOC values and conventional S2 contents was established, as shown in Equation 2.

$$S2c = a2 \times TOC + b2 \times S2 + c2 \quad (2)$$

Where, S2c is measured by multistep pyrolysis and represents the content of adsorbed hydrocarbons, mg/g. TOC is the total organic carbon of the sample, %. S2 is measured by conventional pyrolysis and represents the pyrolyzed hydrocarbons containing adsorbed hydrocarbons, mg/g. a2, b2, c2 are the correlation coefficients, dimensionless. In this model, a2, b2, and c2 are 0.102, 0.692, and -0.359, respectively.

Step 3: Integrated calibration. The actual S1 content of shale in the subsurface ($S1_0$) should include the measured S1 content, light hydrocarbon lost before pyrolysis analysis ($S1_l$), and adsorbed hydrocarbon detected as S2 (S2c). The actual S2 ($S2_0$) content in subsurface shale should be obtained by subtracting the adsorbed hydrocarbon from conventional pyrolysis S2.

$$S1_0 = S1c + S2c \quad (3)$$

$$S2_0 = S2\text{-}S2c \quad (4)$$

where $S1_0$ is the original generated hydrocarbons, mg/g; $S2_0$ is the original pyrolyzed hydrocarbons, mg/g; S1c is measured by freeze–thaw pyrolysis, and represents the free hydrocarbons before the loss of light hydrocarbons, mg/g; S2c is measured by multistep pyrolysis, and represents the content of adsorbed hydrocarbons, mg/g; S2 is measured by conventional pyrolysis and represents the content of adsorbed hydrocarbons, mg/g.

Appendix B

Theoretical foundation and calculation steps of hydrocarbon micromigration evaluation [19,56].

Based on the mass balance principle, the shale oil content is controlled by hydrocarbon intramicromigration (HIM) and hydrocarbon extramicromigration (HEM). The real hydrocarbon generation potential (HGP_R) of shales can be characterized by a hydrocarbon generation potential index.

$$HGP_R = (S_{1R} + S_{1I} + S_{1E} + S_2)/TOC \times 100 \quad (1)$$

where S_{1R} is the residual hydrocarbon amount, S_{1I} is the HIM amount, S_{1E} is the HEM amount, and S_2 is the remaining hydrocarbon generation potential.

Compared to the original hydrocarbon generation potential (HGP_0). The following three situations exist:

1) Neither HIM nor HEM occurred. In this case, both S_{1I} and S_{1E} are 0, and all generated hydrocarbons (S_{1R}) are retained in shale, as shown below:

$$HGP_R = HGP_0 \quad (2)$$

$$HGP_R = (S_{1R} + S_2)/TOC \times 100 \quad (3)$$

2) HIM occurred without HEM. In this case, $S_{1E} = 0$, and $S_{1I} > 0$; all generated hydrocarbons (S_{1R}) are retained in shale, and thus, $HGP_R > HGP_0$, as shown below:

$$HGP_R > HGP_0 \quad (4)$$

$$HGP_R = (S_{1R} + S_{1I} + S_2)/TOC \times 100 \quad (5)$$

3) HEM occurred without HIM. Hydrocarbon expulsion occurs only when the hydrocarbon generation amount satisfies self-adsorption, pore water dissolution, oil dissolution (gas), capillary saturation, and other forms of residual occurrences of shale cells. Due to the entirely oil-saturated state of shale cells, HEM occurs; therefore, $S_{1E} > 0$, $S_{1I} = 0$, and $HGP_R < HGP_0$, as shown below:

$$HGP_R < HGP_0 \quad (6)$$

$$HGP_R = (S_{1R} + S_2)/TOC \times 100 \quad (7)$$

According to the mass balance principle, the micromigrated hydrocarbons (ΔQ) of shales can be evaluated, as shown below:

$$\Delta Q = HGP_0 - HGP_R \quad (8)$$

$\Delta Q < 0$ indicates HIM, and $\Delta Q > 0$ indicates HEM. The greater the absolute values are, the greater the HIM and HEM amounts are.

Since most pyrolysis data were tested after hydrocarbon expulsion occurred and since the TOC content changes during thermal evolution, the hydrocarbon generation potential measured currently must be restored to its original state. Kerogen kinetics is important in resource evaluation for better understanding the thermal maturation process of source rocks, and the relationship between HI and Tmax demonstrates the kinetic behavior of the shales, which is often expressed as hydrocarbon transformation ratio. The data-driven model to reconstruct the original hydrogen index (HI_0), representing the HGP_0, as shown below:

$$HI = HI_0\left\{1 - \exp\left[-\left(\frac{T_{max}}{\beta}\right)^{\theta}\right]\right\} + c \quad (9)$$

$$T_R = \frac{1200}{HI_0}\frac{(HI_0 - HI)}{(1200 - HI)} \quad (10)$$

where HI_0 is the original HI, in mg HC/g TOC; HI is the hydrogen index ($S_2/TOC \times 100$, in mg HC/g TOC); T_R is the kerogen transformation rate, in %; β and θ are unknown parameters specific to kerogen kinetics; and C is a constant indicating the error magnitude in the measured hydrogen index at a very high Tmax.

The measured Tmax and hydrogen index (HI) from Dongpu Depression shale were fitted with a data-driven model. To obtain a more accurate hydrocarbon conversion process, first classified organic matter types and then simulated the reaction paths of the hydrocarbon generation kinetics of different kerogen types. The HI evolution model and kerogen transformation rate (T_R) of different shale types under different maturity levels were established. The following four situations exist:

$$\text{Type I}: HI = 735\left\{1 - \exp\left[-\left(\frac{T_{max}}{438}\right)^{-49}\right]\right\} \quad (11)$$

$$\text{Type II}_1: \text{HI} = 385\left\{1 - \exp\left[-\left(\frac{T_{max}}{445}\right)^{-45}\right]\right\} \quad (12)$$

$$\text{Type II}_2: \text{HI} = 210\left\{1 - \exp\left[-\left(\frac{T_{max}}{441}\right)^{-33}\right]\right\} \quad (13)$$

$$\text{Type III}: \text{HI} = 95\left\{1 - \exp\left[-\left(\frac{T_{max}}{436}\right)^{-31}\right]\right\} \quad (14)$$

Then, HI was calculated at different maturities, and kerogen TR models of kerogens of different types were obtained. The HI_0 values of shales with specific organic matter types were obtained by combining the calculated T_R and HI, that is, HGP_0. Finally, ΔQ was obtained by subtracting HGP_R from HGP_0.

Data availability

Data will be made available on request.

References

[1] Hughes JD. Energy: A reality check on the shale revolution. Nature 2013;494 (7437):307. https://doi.org/10.1038/494307a.12.

[2] Hopkins AS. The next energy economy. Science 2017;356(6339):709. https://doi.org/10.1126/science.aam8696.

[3] EIA. Technically Recoverable Shale Oil and Shale Gas Resources: An assessment of shale Formation in countries outside the United States, Washington 2013.

[4] Zou CN, Yang Z, Cui JW, Zhu RK, Hou LH, Tao SZ, et al. Formation mechanism, geological characteristics and development strategy of nonmarine shale oil in China. Pet Explor Dev 2013;40(1):15–27. https://doi.org/10.1016/S1876-3804(13)60002-6.

[5] Zou CN, Zhu RK, Chen ZQ, Ogg JG, Wu ST, Dong DZ, et al. Organic-matter-rich shales of China. Earth Sci Rev 2019;189:51–78. https://doi.org/10.1016/j.earscirev.2018.12.002.

[6] Zhao WZ, Hu SY, Hou LH, Yang T, Li X, Guo BC, et al. Types and resource potential of continental shale oil in China and its boundary with tight oil. Pet Explor Dev 2020;47(1):1–11. https://doi.org/10.1016/S1876-3804(20)60001-5.

[7] Zou CN, Ma F, Pan SQ, Zhang XS, Wu ST, Fu GY, et al. Formation and distribution potential of global shale oil and the developments of continental shale oil theory and technology in China. Earth Sci F 2023;30(01):128–42. in Chinese with English abstract.

[8] Hu T, Pang XQ, Jiang FJ, Zhang CX, Wu GY, Hu ML, et al. Dynamic continuous hydrocarbon accumulation (DCHA): Existing theories and a new unified accumulation model. Earth Sci Rev 2022;232:104109. https://doi.org/10.1016/j.earscirev.2022.104109.

[9] Hu T, Pang XQ, Jiang FQ, Wang QF, Liu XH, Wang Z, et al. Movable oil content evaluation of lacustrine organic-rich shales: Methods and a novel quantitative evaluation model. Earth Sci Rev 2021;214:103545. https://doi.org/10.1016/j.earscirev.2021.103545.

[10] Pang XQ, Li M, Li BY, Wang T, Hui SS, Liu Y, et al. Main controlling factors and movability evaluation of continental shale oil. Earth Sci Rev 2023;243:104472. https://doi.org/10.1016/j.earscirev.2023.104472.

[11] Jarvie DM. Shale resource systems for oil and gas: part 2: Shale-oil resource systems. Shale reservoirs-giant resources for the 21st century. AAPG Mem 2012;97:89–119. https://doi.org/10.1306/13321447M973489.

[12] Jarvie DM. Components and processes affecting producibility and commerciality of shale resource systems. Geol Acta 2014;12(4):307–25. https://doi.org/10.1344/GeologicaActa2014.12.4.3.

[13] Kuhn PP, Di PR, Hill R, Lawrence JR, Horsfield B. Three-dimensional modeling study of the low-permeability petroleum system of the Bakken Formation. AAPG Bull 2012;96(10):1867–97. https://doi.org/10.1306/03261211063.

[14] Larter SR, Huang HP, Snowdon L. What we do not know about self-sourced oil reservoirs: challenges and potential solutions. In: SPE 2012; 162777, pp. 1–4. https://doi.org/10.2118/162777-MS.

[15] Lu SF, Huang WB, Chen FW, Li JJ, Wang M, Xue HT, et al. Classification and evaluation criteria of shale oil and gas resources: Discussion and application. Pet Explor Dev 2012;39(02):249–56. https://doi.org/10.1016/S1876-3804(12)60042-1.

[16] Lu SF, Xue HT, Wang M, Xiao DS, Huang WB, et al. Several key issues and research trends in evaluation of shale oil. Acta Pet Sin 2016;37(10):1309–22. https://doi.org/10.7623/syxb201610012. in Chinese with English abstract.

[17] Katz B, Lin F. Lacustrine basin unconventional resource plays: Key differences. Mar Pet Geol 2014;56:255–65. https://doi.org/10.1016/j.marpetgeo.2014.02.013.

[18] Hu T, Jiang FJ, Pang XQ, Liu Y, Wu GY, Zhou K, et al. Identification and evaluation of shale oil micro-migration and its petroleum geological significance. Pet Explor Dev 2024;51(1):114–26. https://doi.org/10.1016/S1876-3804(24)60010-8.

[19] Hu T, Liu Y, Jiang FJ, Pang XQ, Wang QF, Zhou K, et al. A novel method for quantifying hydrocarbon micromigration in heterogeneous shale and the controlling mechanism. Energy 2024;288:129712. https://doi.org/10.1016/j.energy.2023.129712.

[20] Han YJ, Mahlstedt N, Horsfield B. The Barnett Shale: Compositional fractionation associated with intraformational petroleum migration, retention, and expulsion. AAPG Bull 2015;99(12):2173–202. https://doi.org/10.1306/06231514113.

[21] Xi KL, Li K, Cao YC, Lin M, Niu XB, Zhu RK, et al. Laminae combination and shale oil enrichment patterns of Chang 73 sub-member organic-rich shales in the Triassic Yanchang Formation, Ordos Basin NW China. Pet Explor Dev 2020;47(6):1244–55. https://doi.org/10.1016/S1876-3804(20)60142-8.

[22] Guo QL, Yao Y, Hou LH, Tang SH, Pan SQ, Yang F, et al. Oil migration, retention, and differential accumulation in "sandwiched" lacustrine shale oil systems from the Chang 7 member of the Upper Triassic Yanchang Formation, Ordos Basin. China Inter J Coal Geo 2022;261:104077. https://doi.org/10.1016/j.coal.2022.104077.

[23] Edman JD, Pitman JK. Geochemistry of Eagle Ford group source rocks and oils from the First Shot Field Area. Texas AAPG Bull 2010;60:217–34.

[24] Gao ZY, Bai LX, Hu QH, Yang Z, Jiang ZX, Wang ZW, et al. Shale oil migration across multiple scales: A review of characterization methods and different patterns. Earth Sci Rev 2024;104819. https://doi.org/10.1016/j.earscirev.2024.104819.

[25] Wang M, Wilkins RWT, Song GQ, Zhang LY, Xu XY, Li Z, et al. Geochemical and geological characteristics of the Es_3^L lacustrine shale in the Bonan sag, Bohai Bay Basin. China Int J Coal Geol 2015;138:16–29. https://doi.org/10.1016/j.coal.2014.12.007.

[26] Li TW, Jiang ZX, Li Z, Wang PF, Xu CL, Liu GH, et al. Continental shale pore structure characteristics and their controlling factors: a case study from the lower third member of the Shahejie Formation, Zhanhua sag, Eastern China. J Nat Gas Sci Eng 2017;45:670–92. https://doi.org/10.1016/j.jngse.2017.06.005.

[27] Hu T, Pang XQ, Jiang S, Wang QF, Zheng XW, Ding XG, et al. Oil content evaluation of lacustrine organic-rich shale with strong heterogeneity: A case study of the Middle Permian Lucaogou Formation in Jimusaer Sag, Junggar Basin. NW China Fuel 2018;221:196–205. https://doi.org/10.1016/j.fuel.2018.02.082.

[28] Huo ZP, Tang X, Meng QK, Zhang JC, Li CR, Yu XF, et al. Geochemical characteristics and hydrocarbon expulsion of lacustrine marlstones in the Shulu Sag, Bohai Bay Basin, Eastern China: assessment of tight oil resources. Nat Resour Res 2020;29:2647–69. https://doi.org/10.1007/s11053-019-09580-8.

[29] Li WH, Lu SF, Xue HT, Zhang PF, Hu Y. Oil content in argillaceous dolomite from the Jianghan Basin, China: Application of new grading evaluation criteria to study shale oil potential. Fuel 2015;143:424–9. https://doi.org/10.1016/j.fuel.2014.11.080.

[30] Wang EZ, Li CR, Feng Y, Song YC, Guo TL, Li MW, et al. Novel method for determining the oil moveable threshold and an innovative model for evaluating the oil content in shales. Energy 2022;239:121848. https://doi.org/10.1016/j.energy.2021.121848.

[31] Wang EZ, Feng Y, Guo TL, Li MW. Oil content and resource quality evaluation methods for lacustrine shale: A review and a novel three-dimensional quality evaluation model. Earth Sci Rev 2022;232:104134. https://doi.org/10.1016/j.earscirev.2022.104134.

[32] Hunt JM. Generation and migration of petroleum from abnormally pressured fluid compartments. AAPG Bull 1990;74(1):1–12. https://doi.org/10.1029/JB095iB01p00649.

[33] Mackenzie AS, Leythaeuser D, Muller P, Quigley TM, Radke M. The movement of hydrocarbons in shales. Nature 1988;331(6151):63–5. https://doi.org/10.1038/331063a0.

[34] Raji M, Gröcke DR, Greenwell HC, Gluyas JG, Cornford C. The effect of interbedding on shale reservoir properties. Mar Pet Geol 2015;67:154–69. https://doi.org/10.1016/j.marpetgeo.2015.04.015.

[35] Zhang TW, Fu QL, Sun X, Hackley PC, Ko LTW, Shao DY. Meter-scale lithofacies cycle and controls on variations in oil saturation, Wolfcamp A. Delaware and Midland Basins AAPG Bull 2021;105(9):1821–46. https://doi.org/10.1306/01152120065.

[36] Zhi DM, Tang Y, He WJ, Guo XG, Zheng ML, Huang LL. Orderly coexistence and accumulation models of conventional and unconventional hydrocarbons in Lower Permian Fengcheng Formation, Mahu sag, Junggar Basin. Pet Explor Dev 2021;48(1):38. https://doi.org/10.1016/S1876-3804(21)60004-6.

[37] Li GX, Zhu RK, Zhang YS, Chen Y, Cui JW, Jiang YH, et al. Geological characteristics, evaluation criteria and discovery significance of Paleogene Yingxiongling shale oil in Qaidam Basin. NW China Pet Explor Dev 2022;49(1):21–36. https://doi.org/10.1016/S1876-3804(22)60002-8.

[38] Cui JW, Zhang ZY, Liu GL, Zhang Y, Qi YL. Breakthrough pressure anisotropy and intra-source migration model of crude oil in shale. Mar Petro Geo 2022;135:105433.https://doi.org/10.1016/j.marpetgeo.2021.105433.
[39] Pang B, Chen JQ, Pang XQ, Hu T, Sheng Y. Driving forces and their relative contributions to hydrocarbon expulsion from deep source rocks: A case of the Cambrian source rocks in the Tarim Basin. Petro Sci 2023;20(1):20–33. https://doi.org/10.1016/j.petsci.2022.08.011.
[40] Sandvik EI, Young WA, Curry DJ. Expulsion from hydrocarbon sources: the role of organic absorption. Org Geochem 1992;19(1e3):77–87. https://doi.org/10.1016/0146-6380(92)90028-V.
[41] Leythaeuser D, Schaefer RG, Radke M. Geochemical effects of primary migration of petroleum in Kimmeridge source rocks from Brae field area, North Sea. I: Gross composition of C15+-soluble organic matter and molecular composition of C15+-saturated hydrocarbons. Geochimi Cosmochim Ac 1988;52(3):701–13. https://doi.org/10.1016/0016-7037(88)90331-6.
[42] Jubb AM, Hackley PC, Hatcherian JJ, Qu J, Nesheim TO. Nanoscale molecular fractionation of organic matter within unconventional petroleum source beds. Energy Fuels 2019;33(10):9759–66. https://doi.org/10.1021/acs.energyfuels.9b02518.
[43] Wu LY, Zhang ZL, Yan RQ, Teng YM, Li B, Hu SL. National Standard of the People's Republic of China: Rock pyrolysis analysis. Beijing: Standard Press of China; 2012.
[44] Jiang QG, Li MW, Qian MH, Li ZM, Li Z, Huang ZK, et al. Quantitative characterization of shale oil in different occurrence states and its application. Petro Geo Exp 2016;06:842–9. in Chinese with English abstract.
[45] Xu GJ, Gao Y, Dong SH, Wang DL,. National Standard of the People's Republic of China: Determination of total organic carbon in sedimentary rock (GB/T 19145-2003). Standard Press of China 2003; Beijing. (in Chinese with English abstract).
[46] Zeng L, Wan MX, Li XH, Jiao YG, Cui SN, Dong XD, et al. Oil and gas industry standard of the People's Republic of China: Analysis method for clay minerals and ordinary non-clay mineralsin sedimentary rocks by the X-ray diffraction (SY/T 5163-2018). Petroleum Industry Press 2018; Beijing. (in Chinese with English abstract).
[47] Wei GZ, Zhu DS, Liu WX. Oil and gas industry standard of the People's Republic of China: Analytical method of rock sample by scanning electron microscope (SY/T5162-2014). Petroleum Industry Press 2014; Beijing. (in Chinese with English abstract).
[48] Lv CY, Qu YT, Chen XJ. Oil and gas industry standard of the People's Republic of China: Measurement of rock pore structure method of image analysis (SY/T6103-2004). Petroleum Industry Press 2004; Beijing. (in Chinese with English abstract).
[49] Ba LQ, Li GY, Tao C. National Standard of the People's Republic of China: Organic geochemical analysis method for geological samples-Part 2: Determination of organic carbon stable isotopic component Isotopic mass spectrometry (GB/T 18340.2-2010). Standard Press of China 2010; Beijing. (in Chinese with English abstract).
[50] Liang S, Zhang Q, Cao Y. National Standard of the People's Republic of China: Organic geochemical analysis method for geological samples-Part 5: Analysis of saturated hydrocarbons in rock extracts and crude oils-Gas chromatograph (GB/T 18340.5-2010). Standard Press of China, 2010; Beijing. (in Chinese with English abstract).
[51] Wang M, Ma R, Li JB, Lu SF, Li CM, Guo ZQ, et al. Occurrence mechanism of lacustrine shale oil in the Paleogene Shahejie Formation of jiyang depression, Bohai Bay Basin. China Pet Explor Dev 2019;46(4):833–46. https://doi.org/10.1016/S1876-3804(19)60242-9.
[52] Hu T, Pang XQ, Xu TW, et al. Identifying the key source rocks in heterogeneous saline lacustrine shales: Paleogene shales in the Dongpu depression, Bohai Bay Basin, eastern China. AAPG Bull 2022;106(6):1325–56. https://doi.org/10.1306/01202218109.
[53] Xu YL, Hu T, Xiao HY, Yuan M, Li LX, Xiong ZM, et al. Characteristics of pore structure and the evolution process in terrestrial shale reservoirs: A case study of the Shahejie Formation in Dongpu Depression, Bohai Bay Basin. ACS Omega 2024;9(46):45943–60. https://doi.org/10.1021/acsomega.4c05540.
[54] Zeng L, Su H, Tang X, Li CR, Jiang S, Wang QF, et al. Fractured tight sandstone oil and gas reservoirs: A new play type in the Dongpu depression, Bohai Bay Basin. China AAPG Bull 2013;97:363–77. https://doi.org/10.1306/09121212057.
[55] Ji H, Li SM, Greenwood P, Greenwood P, Zhang HA, Pang XQ, et al. Geochemical characteristics and significance of heteroatom compounds in lacustrine oils of the Dongpu Depression (Bohai Bay Basin, China) by negative-ion Fourier transform ion cyclotron resonance mass spectrometry. Mar Petrol Geol 2018;97:568–91. https://doi.org/10.1016/j.marpetgeo.2018.07.035.
[56] Wu YQ, Jiang FJ, Hu T, Xu YL, Guo J, Xu TW, et al. Shale oil content evaluation and sweet spot prediction based on convolutional neural network. Mar Petro Geo 2024;167:106997. https://doi.org/10.1016/j.marpetgeo.2024.106997.
[57] Xu TW, Zhang HA, Li JD, Zhao W. Characters of hydrocarbon generation and accumulation of salt-lake facies in Dongpu Sag, Bohai Bay Basin. Oil Gas Geo 2019;40(02):248–61. in Chinese with English abstract.
[58] Li YF, Zeng X, Cai JG, Wang XY, Mu XS, Zhang YX. Mudrocks lithofacies characteristics and North-South hydrocarbon generation difference of the Shahejie Formation in the Dongpu sag. Minerals 2021;11:535. https://doi.org/10.3390/min11050535.
[59] Hackley PC, Zhang TW, Jubb AM, Valentine BJ, Dulong FT, Hatcherian JJ. Organic petrography of Leonardian (Wolfcamp A) mudrocks and carbonates, Midland Basin, Texas: The fate of oil-prone sedimentary organic matter in the oil window. Mar Pet Geol 2020;112:104086. https://doi.org/10.1016/j.marpetgeo.2019.104086.
[60] Walters CC, Gong C, Sun X, Zhang TW. Geochemistry of oils and condensates from the lower Eagle Ford formation, South Texas. Part 3: Basin modeling. Mar Pet Geol 2023;150:106117. https://doi.org/10.1016/j.marpetgeo.2023.106117.